Artificial Neural Network Nonlinear Equalizer for Coherent Optical OFDM

Mutsam A. Jarajreh, Elias Giacoumidis, Ivan Aldaya, Son Thai Le, Athanasios Tsokanos, Zabih Ghassemlooy, and Nick J. Doran

***Abstract*— We propose a novel low-complexity artificial neural network (ANN)-based nonlinear equalizer (NLE) for coherent optical orthogonal frequency-division multiplexing (CO-OFDM) and compare it with the recent inverse Volterra-series transfer function (IVSTF)-based NLE over up to 1000 km of uncompensated links. Demonstration of ANN-NLE at 80-Gb/s CO-OFDM using 16-quadrature amplitude modulation reveals a *Q*-factor improvement after 1000-km transmission of 3 and 1 dB with respect to the linear equalization and IVSTF-NLE, respectively.**

***Index Terms*— Optical communication, coherent optical fiber transmission, functional link artificial neural networks, nonlinear equalizer, OFDM.**

I. Introduction

COHERENT optical orthogonal frequency-division multiplexing (CO-OFDM) is a high spectral efficient modulation format able to virtually eliminate inter-symbol interference (ISI) caused by the fiber chromatic dispersion (CD) and polarization mode dispersion (PMD) [1]. One major drawback of CO-OFDM systems that hitherto remains unsolved is their vulnerability to fiber nonlinear effects due to the high peak-to-average power ratio (PAPR) of OFDM signals. Several digital signal processing (DSP) techniques have been investigated for nonlinearity compensation. The three most recent and prominent are the digital back propagation (DBP) [2], nonlinearity pre- and post-compensation [3], and the inverse Volterra-series transfer function (IVSTF) equalization [4], [5]. The main disadvantage of DBP is the extensive use of fast Fourier transform (FFT), which results in significant DSP computational complexity. The second method requires a combination of pre- and post-compensation algorithms, whose implementation is complex and presents marginal performance enhancement compared to linear equalization (LE), e.g. <0.5 dB in the Q-factor [3]. IVSTF equalization has been considered as an effective method for combating fiber nonlinearity with reported 1 dB improvement in the Q-factor for 256-Gb/s polarization-division-multiplexed 16-quadrature amplitude modulation (16-QAM) [4], [5]. It is worth noting that IVSTF-NLE can be implemented fully in time domain, in frequency domain, or in combined time-frequency domain. We adopted the last approach for simplicity, since convolutions with the fiber linear impulse response are performed in the frequency domain and squaring operations are carried out in the time domain [4], [5].

For a time and frequency-varying channel, e.g. single-mode fiber (SMF), equalization based on linear filters is a non-optimum classification strategy because of the linear decision boundaries of the filters [6]. An alternative approach would be based on equalizers with nonlinear decision boundaries, such as artificial neural networks (ANNs) based on a multilayer perceptron (MLP). These equalizers perform a complex mapping between input and output spaces, having complex decision regions with nonlinear decision boundaries [7]. ANN has been adopted as an attractive solution for combating nonlinear impairments in wireless communications [7], [8]. However, the application of ANN in optical OFDM for linear and nonlinear impairments compensation has never been reported.

In this letter, a novel versatile ANN-based NLE is presented for a single-polarization 16-QAM CO-OFDM system, which is a first step toward the implementation of an ANN-based NLE for dual-polarization CO-OFDM. The fiber nonlinearity compensation capability is evaluated for up to 80-Gb/s signals over 1000 km of uncompensated link, and a comparison with the benchmark IVSTF-based NLE [4], [5] is provided. Results with ANN-NLE reveal an enhancement with respect to LE of the Q-factor by ∼3 dB at 1000 km of standard SMF (SSMF) transmission. It is also shown that, ANN-based NLE outperforms in Q-factor (up to 2 dB) when compared to the benchmark IVSTF equalization for signals at bit-rates of >40-Gb/s at 1000 km of transmission.

II. Artificial Neural Network Nonlinear Equalizer

The schematic diagram of the proposed ANN-based NLE for the 16-QAM CO-OFDM receiver is depicted in Fig. 1(a), where $s(k)$ is the training vector, *i.e.* the pre-known subcarrier set transmitted during the training stage. Since the CO-OFDM signal consists of k subcarriers ANN-NLE is comprised of k sub-neural networks, with each sub-network

Manuscript received September 15, 2014; revised November 17, 2014; accepted November 21, 2014. Date of publication December 4, 2014; date of current version January 21, 2015. This work was supported by the European Commission through ICT Project DISCUS under Grant 318137 within the 7th Framework Programme.

M. A. Jarajreh and Z. Ghassemlooy are with the Optical Wireless Communications Group, Faculty of Engineering and Environment, University of Northumbria at Newcastle, Newcastle upon Tyne NE1 8ST, U.K. (e-mail: mutsam.jarajreh@gmail.com; z.ghassemlooy@northumbria.ac.uk).

E. Giacoumidis, S. T. Le, and N. J. Doran are with the School of Engineering and Applied Science, Aston Institute of Photonic Technologies, Birmingham B4 7ET, U.K. (e-mail: e.giacoumidis@aston.ac.uk; let1@aston.ac.uk; n.j.doran@aston.ac.uk).

I. Aldaya is with the Department of Electrical and Computational Engineering, Instituto Tecnológico y de Estudios Superiores de Monterrey, Monterrey 64800, Mexico (e-mail: ivan.a.aldaya@ieee.org).

A. Tsokanos is with the School of Computing and Mathematics, Plymouth University, Plymouth, U.K. (e-mail: athanasios.tsokanos@plymouth.ac.uk).

Color versions of one or more of the figures in this letter are available online at http://ieeexplore.ieee.org.

Digital Object Identifier 10.1109/LPT.2014.2375960

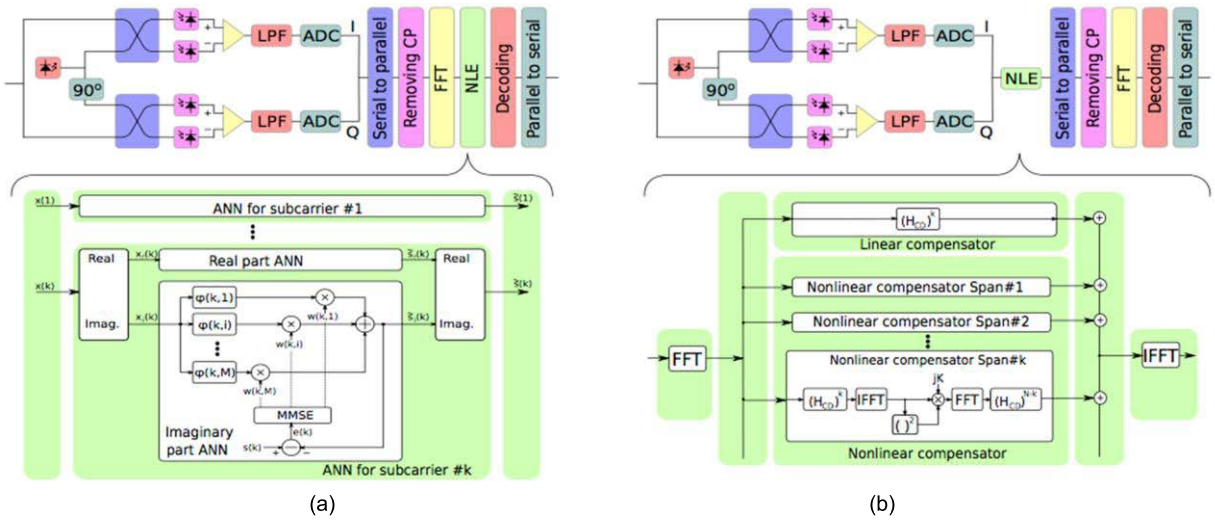

Fig. 1. 16-QAM CO-OFDM receiver block diagram showing the equalization schematic diagrams of (a) the ANN sub-neural network, and (b) the benchmark inverse Volterra-series transfer function (IVSTF) [4], [5]. LPF: low-pass filter; ADC: analog-to-digital converter; CP: cyclic prefix; (I)FFT: (inverse) fast-Fourier transform; NLE: nonlinear equalizer; ANN: artificial neural network; MMSE: minimum mean-square error; H_{CD}: nonlinear system chromatic dispersion.

being associated to each subcarrier. The received symbols for every subcarrier $x(k)$ are fed to NLE neurons where they are multiplied with the weight value for a given OFDM subcarrier and neuron $w(k,i)$. Afterwards, the outputs of the different neurons are summed to generate $\hat{s}(k)$, an estimation of the undistorted signal. In the training stage, the well-known minimum mean-square error (MMSE) algorithm, which is standard in the new feed-forward networks, is used to determine the error signal and update the weights. The weights are iteratively updated until the desired error value is reached, thus indicating the optimum match between the sub-network output and the transmitted (undistorted) OFDM subcarrier symbols. The error signal is given as:

$$e(k) = s(k) - \hat{s}(k) \tag{1}$$

where $\hat{s}(k)$ is calculated in terms of a nonlinear activation function $\varphi(k,i)$, performing the NLE and $w(k,i)$, which is given by:

$$\hat{s}(k) = \sum_{i=1}^{16} w(k,i)\varphi(k,i)s(k). \tag{2}$$

The nonlinear activation function is application dependent and it is mostly required to be a differentiable function. For the proposed ANN-NLE a sigmoid function is used, which can satisfy a conflicting relationship between the boundedness and the differentiability of a complex function. This is called the "split" complex activation function, where two conventional real-valued activation functions process the in-phase and quadrature components.

It is important to mention that the number of neurons in every neural sub-net is equal to the number of the signal modulation format level, which in the case of 16-QAM is 16. In this letter, the ANN-NLE is based on the feed-forward network that uses the Riedmiller's resilient back-propagation (RR-BP) algorithm [9]. The training function updates the weights and the bias values according to the RR-BP algorithm, which is computationally more efficient than other training algorithms, and it performs an approximation to the global minimization achieved by the steepest descent [10]. Hence, as mentioned, RR-BP minimizes the difference between the ANN output and the desired output, *i.e.* the target output. This is achieved in real-time splitting the complex OFDM data into two real-valued data collections; the real $\hat{s}_r(k)$ and imaginary $\hat{s}_i(k)$ parts are fed separately into two ANN sub-networks and the outputs are recombined and given by:

$$\hat{s}_{Final} = \hat{s}_r(k) + j \cdot \hat{s}_i(k) \tag{3}$$

For our numerical investigations, the employed transfer functions for the hidden layer are differentiable and similar to the hyperbolic tangent function, as suggested in [11]. For the output layer, the linear function "purelin" is used. The block identified as MMSE in Fig. 1(a), represents the subsystem that implements the RR-BP algorithm used to find the weights that minimize the error vector (the vector whose k^{th} component is $e(k)$):

$$E(n) = \|S(n) - \hat{S}(n)\|^2 \tag{4}$$

where $S(n)$ and $\hat{S}(n)$ are the desired and calculated output vectors, respectively. The weights are updated according to the following 5 steps by applying gradient descent on the cost function $E(n)$ in order to reach a minimum:

- *Step 1:* Initialize the weights and thresholds to small random numbers.
- *Step 2:* Present the input vector, $X(n)$, and the desired output vector $S(n)$.
- *Step 3:* Calculate $\hat{S}(n)$ from the $X(n)$ and compute the error vector $E(n)$ using (4).
- *Step 4:* Adapt weights based on:

$$w(k,i)_{n+1} = w(k,i)_n - \tilde{n}(\partial \mathrm{E(n)}/\partial w(k,i)'_n) \tag{5}$$

where $w(k,i)_n$ is the weight of the i^{th} neuron of the k^{th} sub-neural network (i^{th} symbol of the k^{th} subcarrier) at the n^{th} iteration, and $\tilde{n}$ is the learning rate parameter. It is worth mentioning that when $\tilde{n}$ is very small, the

algorithm will take long time to converge; whereas, when ñ is too large the system may run into an unstable state.

- *Step 5:* If $E(n)$ is above the threshold, go to *step 2*.

The schematic block diagram of benchmark IVSTF equalizer is depicted in Fig. 1(b), which is similar to that reported in [4] and [5] to account for single-polarization CO-OFDM. Compared to ANN, the IVSTF-NLE is placed just after the ADCs to reduce DSP complexity by means of reducing the number of FFT/IFFT blocks. The IVSTF-NLE inherits some of the features of the hybrid time-and-frequency domain implementation, such as non-frequency aliasing and simple implementation. From Fig. 1(b), it can be clearly identified that CD, *i.e.* $(H_{CD})^k$, and the fiber nonlinearity are combated by the linear and nonlinear compensator tool, respectively. It should be mentioned that for purposes of reduced complexity and processing time, very high order Volterra kernels have not been considered in this letter, thus offering ∼50% reduced computational complexity compared to the single-step/span DBP [5]. The number of operations in IVSTF-NLE is proportional to $N_{sc} \cdot K \cdot log_2(N_{sc} \cdot K)$ with N_{sc} representing the number of subcarriers and K the oversampling factor (4 in our case). On the other hand, the number of operations required by the ANN-NLE is proportional to $N_{sc} \cdot M$, where N_{sc} and M are the number of subcarriers and the number of levels in each dimension of the constellation, respectively. Therefore, since clearly $M < K \cdot log_2(N_{sc} \cdot K)$, ANN-NLE is more efficient from the computational complexity point of view.

III. CO-OFDM System Model

The proposed ANN and benchmark IVSTF equalization schemes were validated by carrying out numerical simulations in a Matlab/VPI-transmission-Maker co-simulation environment (electrical domain in Matlab and optical domain in VPI-*version 9*). For the IVSTF-NLE, we have calculated up to 3rd order Volterra kernels [4], [5]. A CO-OFDM system with homodyne reception was considered using 16-QAM subcarrier modulation and payload bit-rates (BRs) ranging from 40-Gb/s up to 80-Gb/s, before adding the different transmission overheads, *i.e.* the cyclic prefix (CP) and training symbols for channel estimation. A 64-point IFFT/FFT pair was used to reduce the complexity of the ANN-NLE, and 1000 OFDM symbols were simulated. A transmission of up to 1000 km (10 homogeneous spans × 100 km) was considered. A large CP overhead of 25% was added to virtually eliminate the ISI caused by CD and PMD, which also relaxes the synchronization requirements of the CO-OFDM demodulator. The receiver in-phase and quadrature signals were filtered by 2nd-order low-pass filters (LPFs) with a 3-dB bandwidth of BR/6.15 Hz. The simulated Erbium-doped fiber amplifiers (EDFAs) had a noise figure of 6 dB and a gain of 20 dB. Ideal coherent receiver was assumed to focus on the impacts of the fiber-induced nonlinear effects. The digital-to-analog/analog-to-digital converter (DAC/ADC) sampling rate was set to BR/3.2 S/s. The DAC/ADC clipping ratio and quantization have been taken into account and set to 13 dB and 10-bits, respectively, even if they do not have a significant impact on the performance of OFDM for a number of subcarriers >32 [12], [13]. The launched optical power for LE was at the optimum value, −6 dBm. Balanced positive-intrinsic-negative (PIN) photo-detectors with responsivity of 0.9 A/W were used. For the SSMF the following parameters were considered: CD of 17 ps/nm/km, 0.2 dB/km of fiber loss, CD slope of 0.06 ps/km/nm^2, PMD coefficient of 0.1 ps/km$^{0.5}$, a nonlinear Kerr coefficient of 2.6×10^{-20} m^2/W and an effective core area of 80 μm^2. The transceiver parameters for the CO-OFDM transmission model are summarized in Table I.

TABLE I
TRANSCEIVER PARAMETERS

Parameter	Description & Value
Payload bit-rate	40–80 Gb/s
Subcarrier modulation format	16-QAM
Operating wavelength	1550 nm
Number of OFDM subcarriers	64
Cyclic prefix (CP) overhead	25 %
Forward-error-correction overhead	7%
ANN training vector overhead	5%
OFDM frame period	6.4–3.2 ns
Photo-detector type	PIN
DAC/ADC sampling rate	12.5–25 GS/s
DAC/ADC quantization bits	10
DAC/ADC clipping ratio	13 dB
LPF roll-off function	Bessel-Thomson
LPF 3 dB bandwidth (order)	6.5–13 GHz (2nd order)
EDFA gain (noise figure)	20 dB (6 dB)
SSMF span number (length)	10 (100 km)

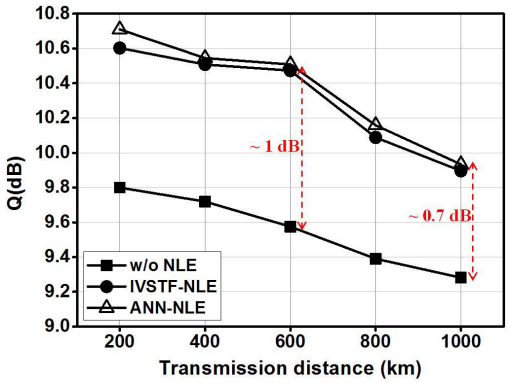

Fig. 2. Q-factor vs. transmission distance for 40-Gb/s CO-OFDM at optimum launched optical power of −6 dBm for IVSTF/ANN-NLEs and without (w/o) using NLE.

IV. Nonlinearity Compensation in CO-OFDM

Nonlinearity compensation capability was assessed based on Q-factor, which was estimated from the bit-error-rate (BER) obtained by error counting after hard-decision decoding. The Q-factor is related to the BER value by: $Q = 20log_{10}\left[\sqrt{2}erfc^{-1}(2BER)\right]$. For a Gray-coded 16-QAM modulation, a 10^{-3} (the commonly adopted threshold for forward error correction [FEC] codes) results in a required Q-factor of 9.8 dB. Fig. 2 shows the Q-factor versus the transmission distance for 40-Gb/s 16-QAM CO-OFDM using ANN-NLE, IVSTF-NLE, or LE (the launched optical power was set to −6 dBm, which was the optimum level for LE). It is shown that ANN-NLE can improve the Q-factor of LE by ∼1 dB and ∼0.7 dB at 600 km and 1000 km transmission-lengths, respectively. Compared to IVSTF-NLE, ANN-NLE offers a similar Q-factor improvement over the entire range. Both NLE approaches increase the reach by 800 km compared to

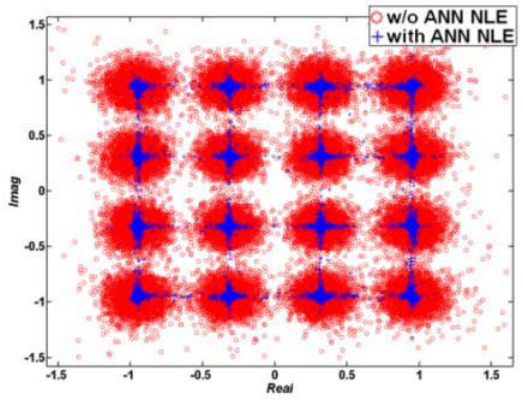

Fig. 3. Received 16-QAM constellation diagram with–w/o ANN-NLE at 600 km of transmission.

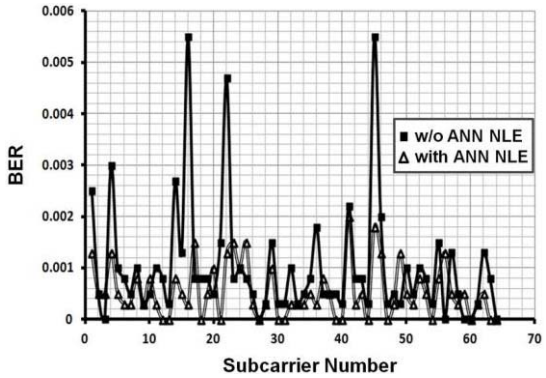

Fig. 4. BER vs. subcarrier index, with–without (w/o) utilizing the ANN-NLE at 600 km of transmission.

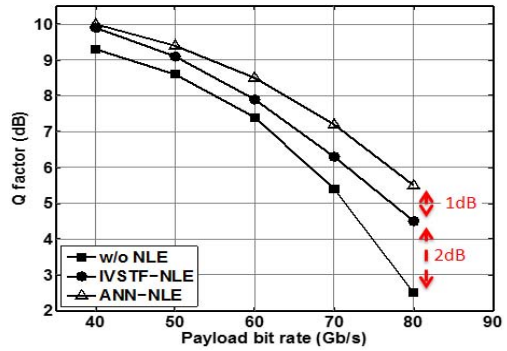

Fig. 5. Q-factor in terms of the payload bit-rate for a 1000-km link without using NLE, using IVSTF-based NLE, and using ANN-NLE.

LE for the targeted Q-factor. The effect of the ANN-based NLE can be observed in Fig. 3, where the constellation diagram of the received signal is depicted at a transmission link of 600 km with and without the ANN-NLE. It can be seen that ANN-NLE has the ability of concentrating the constellation points, reducing the symbol dispersion with respect to LE.

The effect of the ANN-NLE on the BER at each subcarrier is presented in Fig. 4. It can be appreciated that when ANN-NLE was employed, the BER is significantly improved compared to the case when ANN-NLE was excluded due to the reduction of the four-wave mixing (FWM) effect among subcarriers. The performance of LE, IVSTF-NLE, and ANN-NLE for a transmission distance of 1000 km at different payload bit-rates is shown in Fig. 5. Although at 40-Gb/s the performance of ANN-NLE and IVSTF-NLE are similar, ANN-NLE outperforms IVSTF-NLE as bit-rate increases, reaching at a Q-factor improvement of ∼1dB at 80-Gb/s. In comparison to LE, the Q-factor improvement when using ANN-NLE also increases as the bit-rate does, up to ∼3dB for 80-Gb/s; which is an expected result since at higher bit-rates, the nonlinear effects are more significant and, hence, the effect of NLEs is more evident.

V. Conclusion

A novel low-complexity ANN-based NLE has been proposed for CO-OFDM systems. ANN-NLE proved to be a robust nonlinearity DSP technique for up to 80-Gb/s 16-QAM CO-OFDM systems. For 80-Gb/s transmission over 1000-km uncompensated link, ANN-NLE outperforms in terms of Q-factor, LE and IVSTF-NLE by 3 dB and 1 dB, respectively. This letter should trigger the implementation of nonlinear ANN-based equalizers in next generation core networks.

Acknowledgment

The authors would also like to acknowledge the suggestive comments and help of Prof. Andrew D. Ellis from Aston Institute of Photonic Technologies and Miss Eleni Savva for editing from Aston University, School of Languages and Social Sciences, Aston Triangle, Birmingham, B4 7ET, UK.

References

[1] S. L. Jansen, I. Morita, T. C. W. Schenk, N. Takeda, and H. Tanaka, "Coherent optical 25.8-Gb/s OFDM transmission over 4160-km SSMF," *J. Lightw. Technol.*, vol. 26, no. 1, pp. 6–15, Jan. 1, 2008.

[2] G. Gao, J. Zhang, and W. Gu, "Analytical evaluation of practical DBP-based intra-channel nonlinearity compensators," *IEEE Photon. Technol. Lett.*, vol. 25, no. 8, pp. 717–720, Aug. 15, 2013.

[3] A. J. Lowery, "Fiber nonlinearity pre-and post-compensation for long-haul optical links using OFDM," *Opt. Exp.*, vol. 15, no. 20, pp. 12965–12970, 2007.

[4] L. Liu *et al.*, "Intrachannel nonlinearity compensation by inverse volterra series transfer function," *J. Lightw. Technol.*, vol. 30, no. 3, pp. 310–316, Feb. 1, 2012.

[5] E. Giacoumidis *et al.*, "Volterra-based reconfigurable nonlinear equalizer for coherent OFDM," *IEEE Photon. Technol. Lett.*, vol. 26, no. 14, pp. 1383–1386, Jul. 15, 2014.

[6] P. Savazzi, L. Favalli, E. Costamagna, and A. Mecocci, "A suboptimal approach to channel equalization based on the nearest neighbor rule," *IEEE J. Sel. Areas Commun.*, vol. 16, no. 9, pp. 1640–1648, Dec. 1998.

[7] G. Charalabopoulos, P. Stavroulakis, and A. H. Aghvami, "A frequency-domain neural network equalizer for OFDM," in *Proc. IEEE GLOBECOM*, vol. 2. Dec. 2003, pp. 571–575.

[8] S. Rajbhandari, Z. Ghassemlooy, and M. Angelova, "Effective denoising and adaptive equalization of indoor optical wireless channel with artificial light using the discrete wavelet transform and artificial neural network," *J. Lightw. Technol.*, vol. 27, no. 20, pp. 4493–4500, Oct. 15, 2009.

[9] M. Riedmiller and H. Braun, "A direct adaptive method for faster backpropagation learning: The RPROP algorithm," in *Proc. IEEE ICNN*, San Francisco, CA, USA, Mar./Apr. 1993, pp. 586–591.

[10] E. Chen, R. Tao, and X. Zhao, "Channel equalization for OFDM system based on the BP neural network," in *Proc. 8th Int. Conf. Signal Process.*, vol. 3. Beijing, China, 2006, doi: 10.1109/ICOSP.2006.345910.

[11] N. Benvenuto and F. Piazza, "On the complex backpropagation algorithm," *IEEE Trans. Signal Process.*, vol. 40, no. 4, pp. 967–969, Apr. 1992.

[12] E. Giacoumidis, J. L. Wei, X. L. Yang, A. Tsokanos, and J. M. Tang, "Adaptive-modulation-enabled WDM impairment reduction in multi-channel optical OFDM transmission systems for next-generation PONs," *IEEE Photon. J.*, vol. 2, no. 2, pp. 130–140, Apr. 2010.

[13] E. Giacoumidis *et al.*, "Dual-polarization multi-band optical OFDM transmission and transceiver limitations for up to 500 Gb/s uncompensated long-haul links," *Opt. Exp.*, vol. 22, no. 9, pp. 10975–10986, 2014.